Supporting Information

3D Printed, Environment-tolerant All-Solid-State Capacitive Ionic Skin

Yixuan Wu,[a] Ling Cai,[a] Guangxue Chen,[a] Fengzhi Yang,[b] and Minghui He *[a]

[a] State Key Laboratory of Pulp and Paper Engineering, School of Light Industry and Engineering, South China University of Technology, Guangzhou 510640, China
E-mail: heminghui@scut.edu.cn
[b] Zhongshan Qianyou Chemical Materials CO.,LTD, Zhongshan 528400, China
* Corresponding author's E-mail: heminghui@scut.edu.cn

Supplementary Note

Modelling of capacitive sensors. The contact area of SCIS can be divided into two types: real contact area (A_{con}) and suspended area (A_{sus}). The contact area (A) of a SCIS can be divided into 25 sensing unit contact areas (A_{unit}) and 11 suspended area (A_{sus}) (Fig. S8), and each unit cell of the device is defined by two types of areal components: a real contact area A_{con} and a suspended area A_{sus} (Fig. S9).

$$A = 25A_{unit} + 11A_{sus} \tag{1}$$

$$A_{unit} = A_{con} + A_{sus} \tag{2}$$

Hence, the total capacitance of a unit cell (C_{unit}) is composed of a real contact capacitance C_{con} and a suspended capacitance C_{sus}. It is descripted as equation (3).

$$C_{unit} = C_{con} + C_{sus} \tag{3}$$

where C_{con} is the capacitance of the PET dielectric between two PDES electrodes given by

$$C_{con} = C_{PET} = \varepsilon_0 \varepsilon_1 \frac{A_{con}}{d_0} \tag{4}$$

where, ε_0 is the dielectric constant of vacuum (ε_0= 8.85^{-12} F m^{-1}), ε_1 is the relative dielectric constant for the PET layer and d_0 is the initial thickness of the PET dielectric layer.

C_{sus} is the capacitance of the upper-suspended portion given by

$$\frac{1}{C_{sus}} = \frac{1}{C_{PET}} + \frac{1}{C_{air1}} + \frac{1}{C_{air2}} \tag{5}$$

where, C_{PET} is the capacitance of the PET dielectric layer at the suspended portion given by

$$C_{PET} = \varepsilon_0 \varepsilon_1 \frac{A_{sus}}{d_0} \tag{6}$$

C_{air1} and C_{air1} are the capacitance of the upper and lower air gap at the suspended portion respectively given by

$$C_{air1} = \varepsilon_0 \frac{A_{sus}}{d_1} \tag{7}$$

$$C_{air2} = \varepsilon_0 \frac{A_{sus}}{d_2} \tag{8}$$

where d_1 and d_2 are the thickness of the upper and lower air gap ($d_1 = d_2 = 600$ μm), and in this work, it is equal to the line height of the upper and lower electrode structure. Substituting (6), (7) and (8) into (5), we obtain:

$$C_{sus} = \varepsilon_0 \varepsilon_1 \frac{A_{sus}}{d_0 + \varepsilon_{1d_1} + \varepsilon_{1d_2}} \tag{9}$$

Hence, the capacitance of an entire capacitive ionic skin is thus given by

$$C = 25C_{unit} + 11C_{sus} = 25(C_{con} + C_{sus}) + 11C_{sus} = \varepsilon_0 \varepsilon_1 (\frac{25A_{con}}{d_0} + \frac{36A_{sus}}{d_0 + \varepsilon_1 d_1 + \varepsilon_1 d_2})$$

(10)

Supplementary Figures

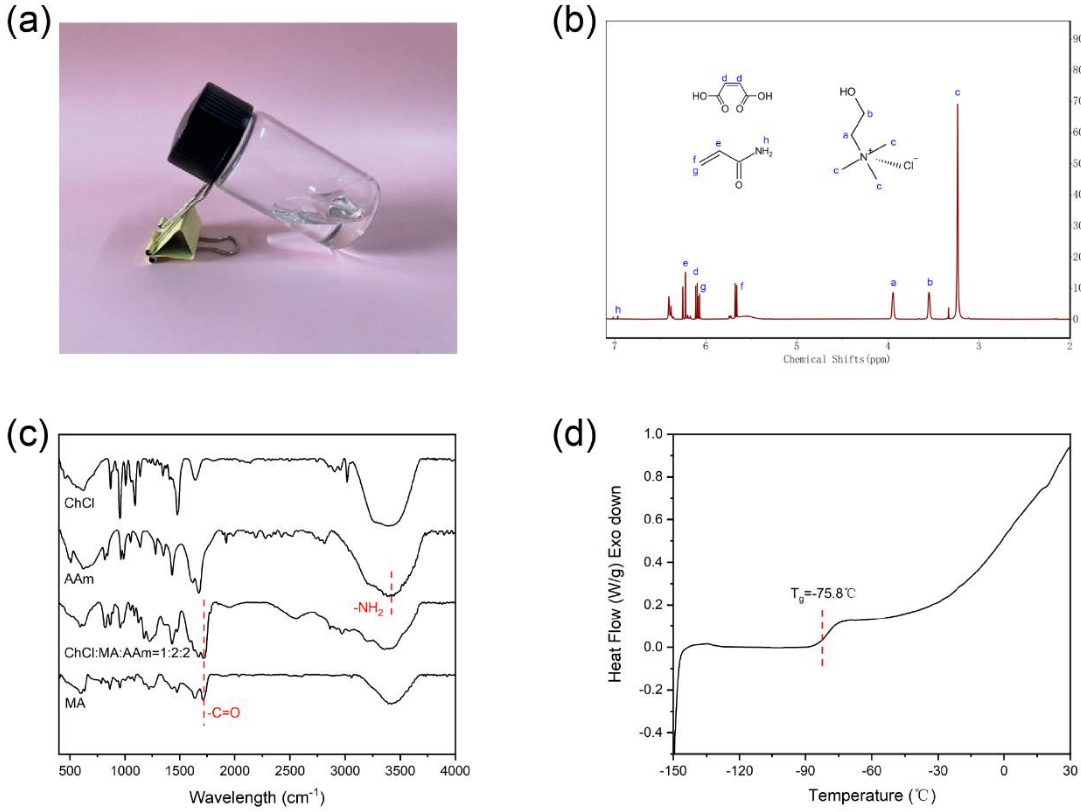

Fig. S1. The preparation and characterization of AAm/ChCl-MA/ChCl type polymerizable deep eutectic solvents (PDES). (a) Digital photographs of transparent AAm/ChCl-MA/ChCl type PDES liquid before polymerization. (b) ^{1}H NMR spectra of AAm/ChCl-MA/ChCl type PDES. The spectrums were recorded using $CDCl_3$ as the external reference. The peak in the spectrum shifts to a lower field due to hydrogen bonding. (c) FTIR spectrums of AAm/ChCl-MA/ChCl type PDES and individual choline-chloride (ChCl), acrylic amide (AAm) and maleic acid (MA). Groups of monomers are present in the spectra. (d) DSC trace of AAm/ChCl-MA/ChCl type PDES. The T_g point of the mixture is lower than that of the single monomers used to synthesis PDES.

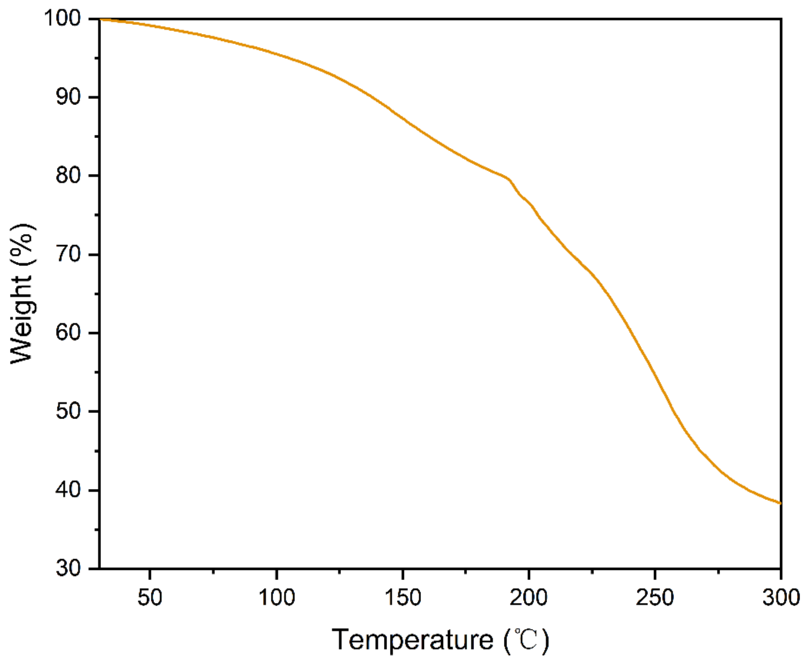

Fig. S2. The thermogravimetric analysis curve of SCIS.

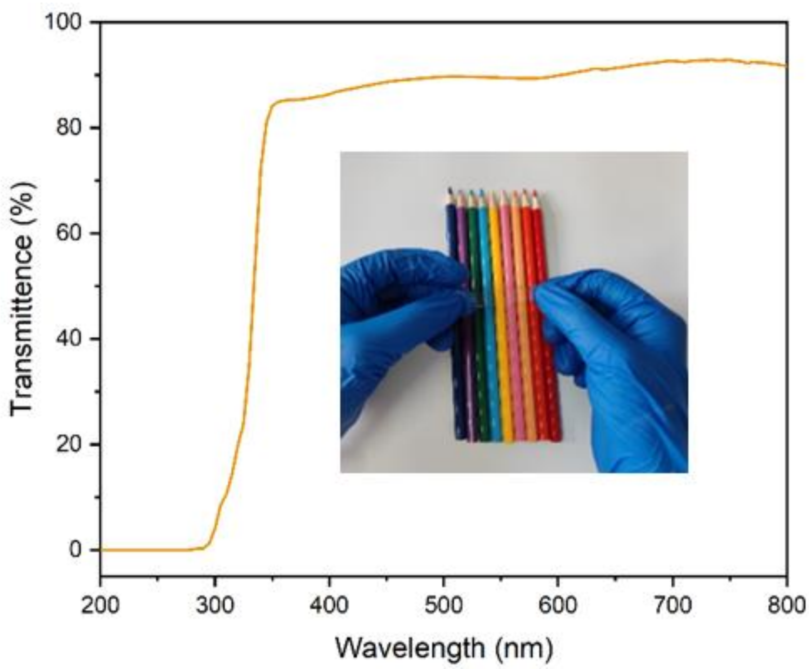

Fig. S3. Digital optical image of a poly(AAm/ ChCl-co-MA/ChCl) elastomer film. It is highly transparent and stretchable.

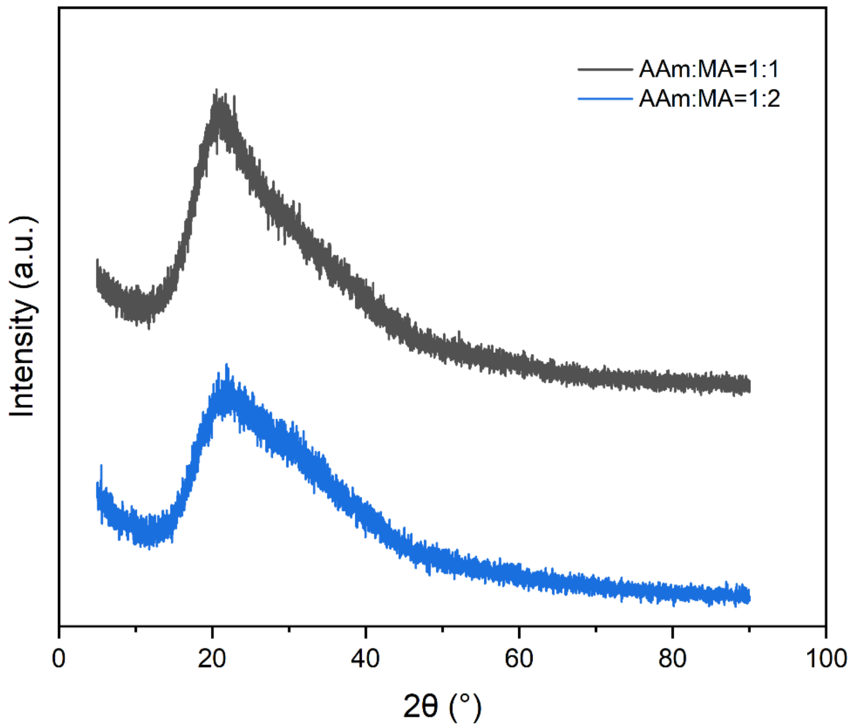

Fig. S4. X-ray diffraction (XRD) spectra.

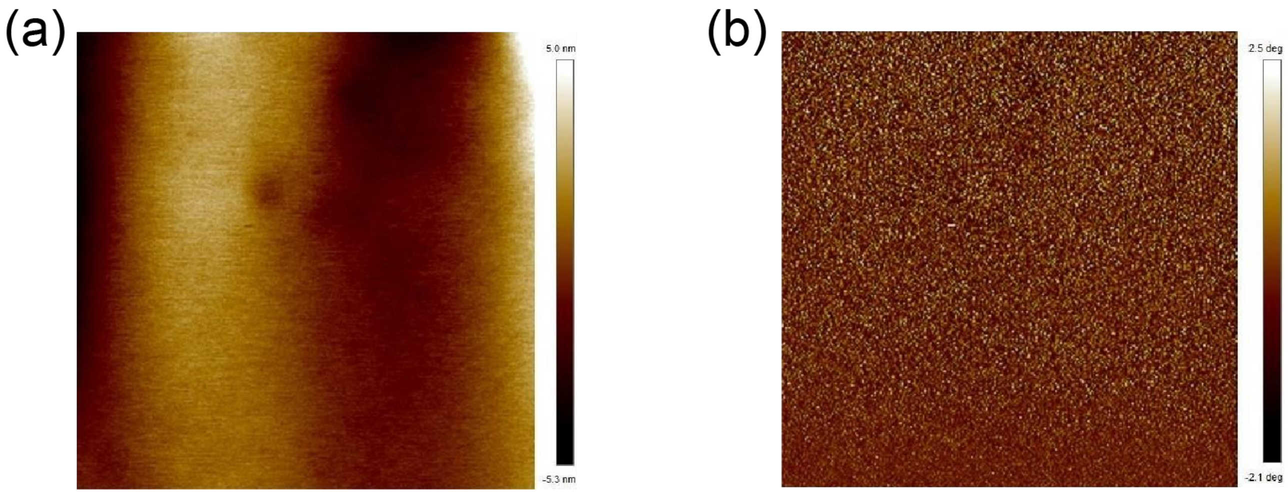

Fig. S5. (a) AFM bitmap of SCIS. (b) AFM phase images of SCIS.

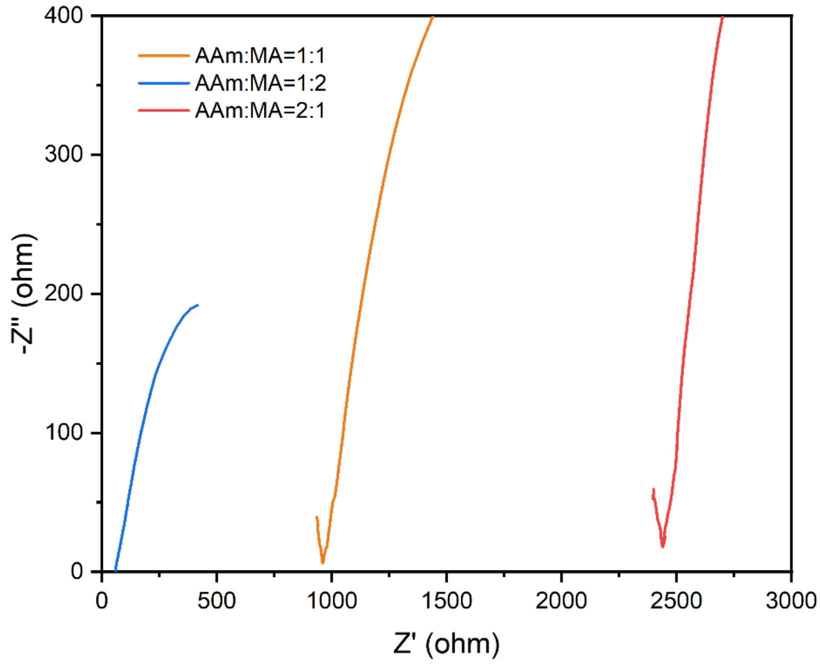

Fig. S6. Electrochemical impedance spectroscopy (EIS) plots of a series of poly(AA/ChCl-co-MA/ChCl) films.

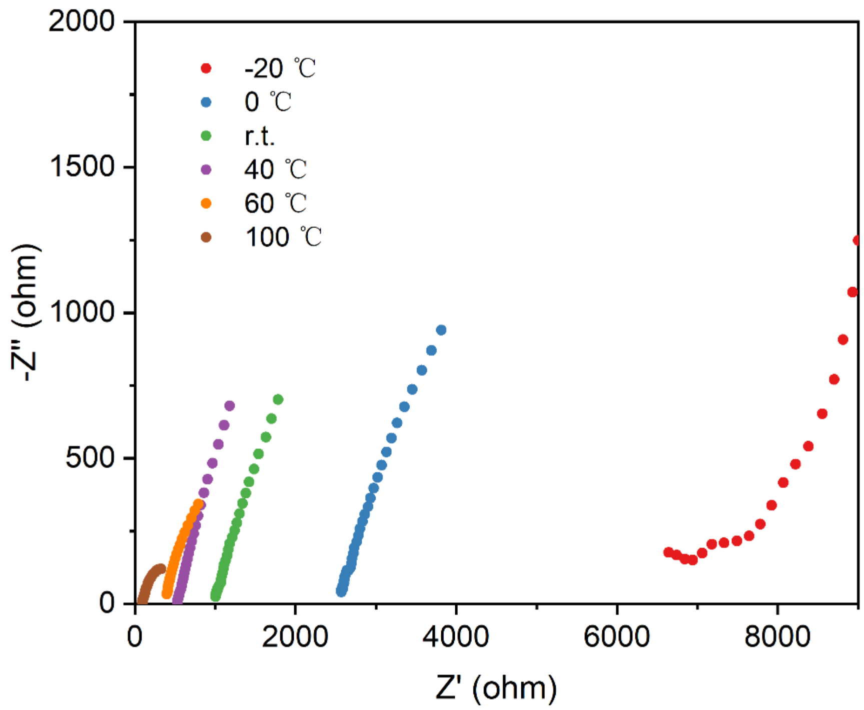

Fig. S7. Electrochemical impedance spectroscopy (EIS) plots of SCIS in different temperature.

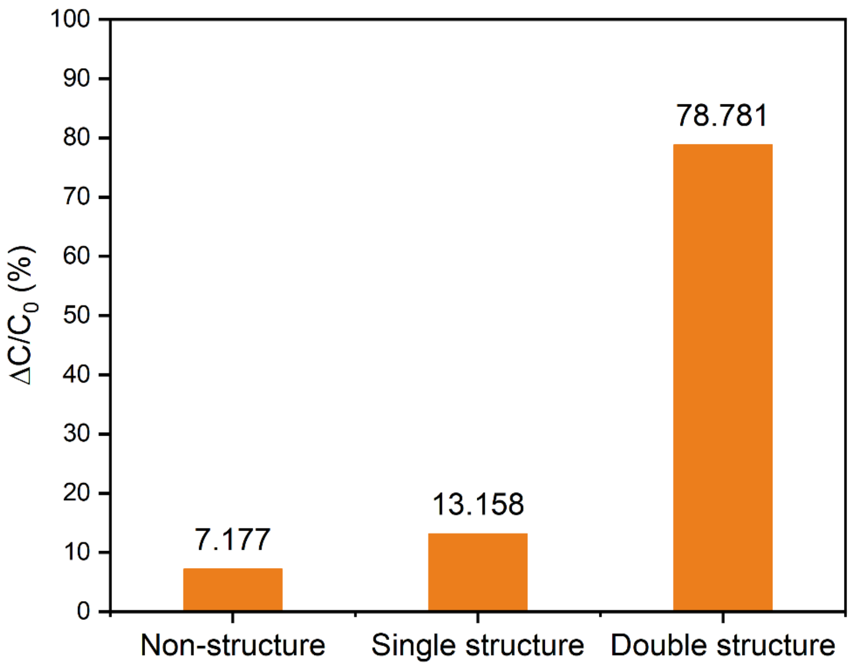

Fig. S8. The change of relative capacitance of ionic skin with different structure.

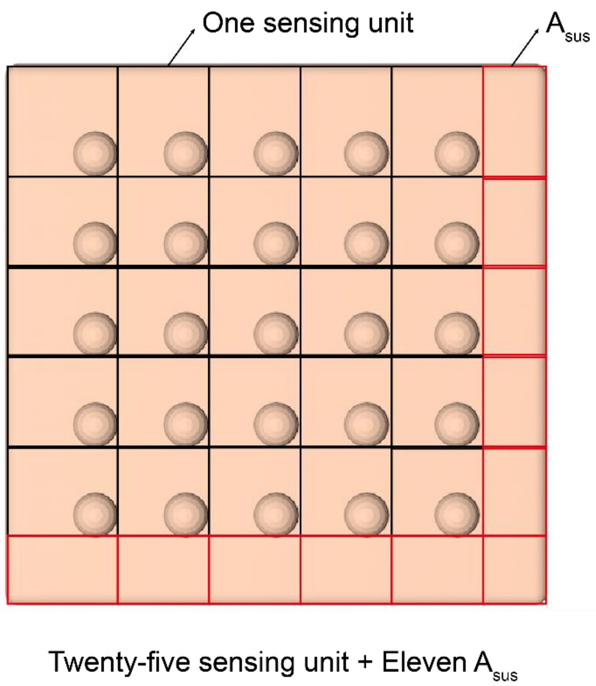

Fig. S9. For a SCIS, it can be divided into 25 sensing unit and 11 suspended unit.

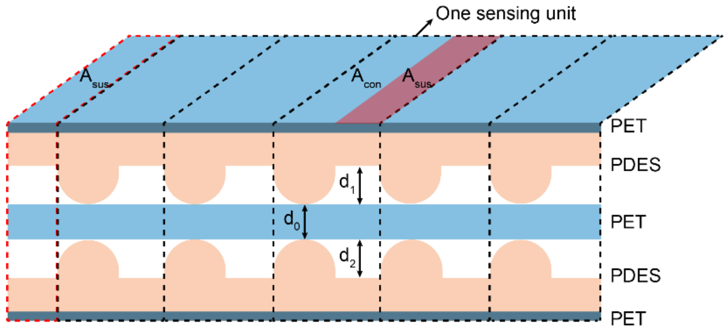

Fig. S10. Each unit cell of the device is defined by two types of areal components: a real contact area A_{con} and a suspended area A_{sus}.

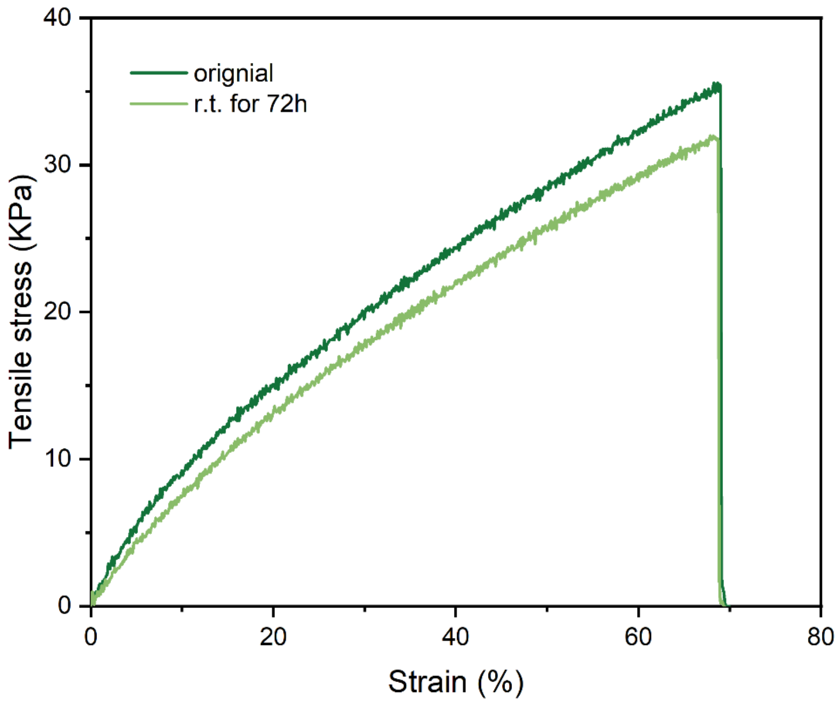

Fig. S11. The stress–strain curves of ionic skin healed in room temperature. Sample width, 14 mm; thickness, 1 mm; gage length, 2 mm. Stretching speed, 10 mm min^{-1}.

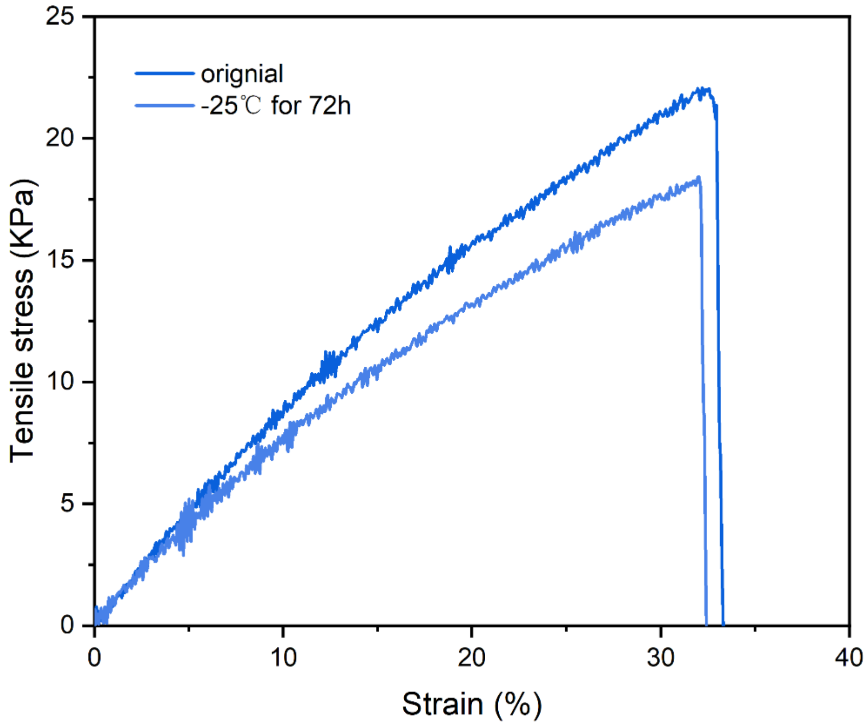

Fig. S12. The stress–strain curves of ionic skin healed in -70℃.

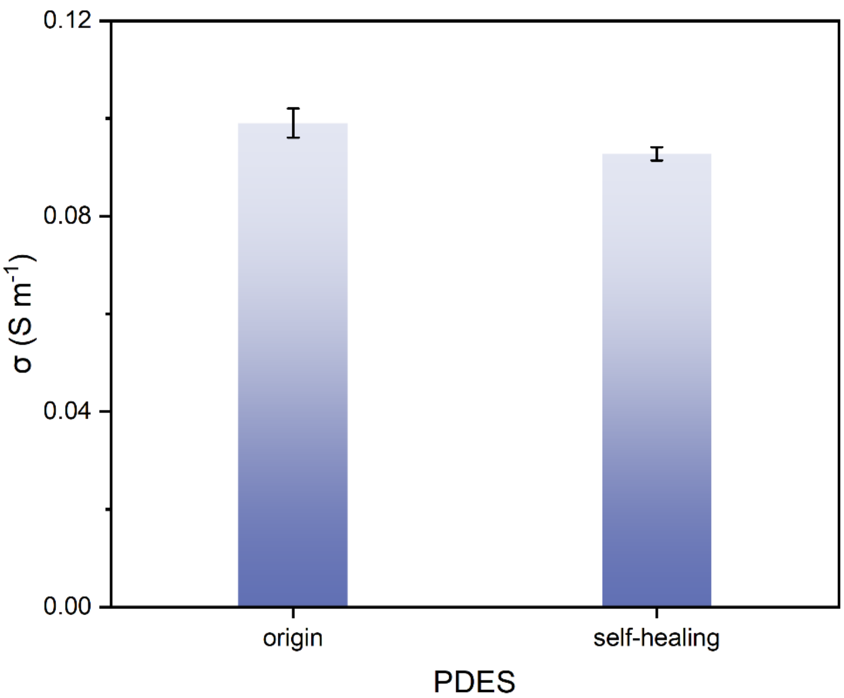

Fig. S13. Electrical conductivity of SCIS before and after self-healing.

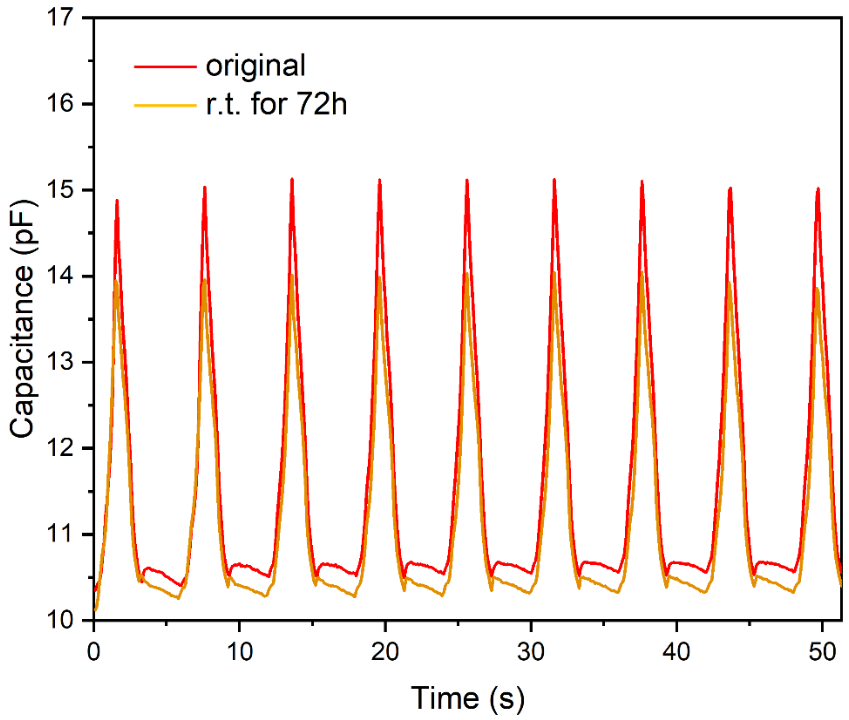

Fig. S14. The sensing performance of SCIS before and after self-healing.